

# Role of Apolipoprotein E in $\beta$ -Amyloidogenesis

## ISOFORM-SPECIFIC EFFECTS ON PROTOFIBRIL TO FIBRIL CONVERSION OF $A\beta$ IN VITRO AND BRAIN $A\beta$ DEPOSITION IN VIVO\*

Received for publication, October 28, 2014, and in revised form, April 22, 2015. Published, JBC Papers in Press, April 27, 2015, DOI 10.1074/jbc.M114.622209

Yukiko Hori<sup>†1</sup>, Tadafumi Hashimoto<sup>†§¶1</sup>, Hidetoshi Nomoto<sup>‡</sup>, Bradley T. Hyman<sup>¶</sup>, and Takeshi Iwatsubo<sup>†§2</sup>

From the <sup>†</sup>Department of Neuropathology and Neuroscience, Graduate School of Pharmaceutical Sciences and the <sup>§</sup>Department of Neuropathology, Graduate School of Medicine, University of Tokyo, Tokyo, 113-0033 Japan and the <sup>¶</sup>Department of Neurology/Alzheimer's Disease Research Unit, Massachusetts General Hospital, Charlestown, Massachusetts 02129

**Background:** *ApoE* is a genetic risk factor for Alzheimer disease.

**Results:** As compared with apoE2/3, apoE4 failed to inhibit the conversion of  $A\beta$  protofibrils to fibrils *in vitro*. Intracerebral injection of  $A\beta$  protofibrils with apoE3 attenuated  $A\beta$  deposition, whereas apoE4 did not.

**Conclusion:** ApoE3, not apoE4, impedes  $\beta$ -amyloid formation.

**Significance:** Interaction between  $A\beta$  and apoE is a critical determinant of  $\beta$ -amyloid formation.

Human *APOE*  $\epsilon 4$  allele is a strong genetic risk factor of Alzheimer disease. Neuropathological and genetic studies suggested that apolipoprotein E4 (apoE4) protein facilitates deposition of amyloid  $\beta$  peptide ( $A\beta$ ) in the brain, although the mechanism whereby apoE4 increases amyloid aggregates remains elusive. Here we show that injection of  $A\beta$  protofibrils induced  $A\beta$  deposition in the brain of APP transgenic mice, suggesting that  $A\beta$  protofibrils acted as a seed for aggregation and deposition of  $A\beta$  *in vivo*. Injection of  $A\beta$  protofibrils together with apoE3 significantly attenuated  $A\beta$  deposition, whereas apoE4 did not have this effect. *In vitro* assays revealed that the conversion of  $A\beta$  protofibrils to fibrils progressed more slowly upon coincubation with apoE2 or apoE3 compared with that with apoE4.  $A\beta$  protofibrils complexed with apoE4 were less stable than those with apoE2 or apoE3. These data suggest that the suppression effect of apoE2 or apoE3 on the structural conversion of  $A\beta$  protofibrils to fibrils is stronger than those of apoE4, thereby impeding  $\beta$ -amyloid deposition.

Alzheimer disease (AD)<sup>3</sup> is pathologically characterized by massive deposition of amyloid  $\beta$  peptides ( $A\beta$ ) as senile plaques in brains. The amyloid hypothesis postulates the central role of  $A\beta$  aggregation as the major cause of neuronal degeneration in AD (1). A subset of AD is inherited as an autosomal dominant trait. Genetic analysis of familial AD (FAD) cases revealed three genes, *A $\beta$  precursor protein (APP)*, *presenilin 1*, and *presenilin*

2, that are causative for FAD (1). Subsequent studies revealed that these mutant genes increase the production of  $A\beta$  or accelerate fibrillization of  $A\beta$ , thereby leading to AD. However, it has not been clarified whether production or fibrillization of  $A\beta$  is up-regulated in the brains of patients with sporadic form of AD, which comprises the major population of AD in the elderly.

A number of non- $A\beta$  proteinaceous components are deposited in senile plaques associated with  $A\beta$  (2). These proteins may interact with  $A\beta$  and modify its deposition in AD brains. The best characterized of these proteins is apolipoprotein E (apoE). ApoE is a 299-amino acid protein secreted from liver into blood plasma, which mediates lipoprotein metabolism. In the central nervous system, apoE is produced and secreted primarily from astrocytes and microglial cells (3–5). Three major polymorphisms in human *apoE* gene, *i.e.*  $\epsilon 2$ ,  $\epsilon 3$ , and  $\epsilon 4$ , that alter the coding of residues 112 and 158 (E2: Cys-112/Cys-158, E3: Cys-112/Arg-158, E4: Arg-112/Arg-158) have been recognized, of which  $\epsilon 4$  is associated with an increased risk for developing AD (6, 7). It has been reported that apoE is codeposited with  $A\beta$  and acquires insolubility along with  $A\beta$  in AD brains (8, 9). Moreover, the density of senile plaques in *APOE*  $\epsilon 4$  homozygous AD patients is higher than those carrying  $\epsilon 3/\epsilon 3$  or  $\epsilon 3/\epsilon 4$  genotypes (10). These studies indicate that apoE proteins, especially apoE4, may be associated with the pathogenesis of AD through interaction with  $A\beta$ . However, the mechanism whereby apoE4 affects  $A\beta$  in the pathogenesis of AD has been unknown.

*In vitro* studies have revealed that formation of  $A\beta$  amyloid fibrils is a complex process, comprised of nucleation and elongation phases (11, 12). In the nucleation phase, seeds are formed from monomer  $A\beta$  through conformational changes. Following the nucleation phase,  $A\beta$  forms fibrils by binding to preformed seeds in the elongation phase. It has been shown that apoE inhibits the nucleation phase of  $A\beta$  fibrillization, although this effect is independent of the apoE isoforms (13, 14). Furthermore, it has not been well understood how apoE affects the  $A\beta$  seeds in the inhibition of nucleation. Along with the classical fibrillization process of  $A\beta$ , a variety of metastable intermediates (*e.g.* paranuclei, protofibrils,  $A\beta$ -derived diffusible ligands)

\* This work was supported by Core Research for Evolutional Science and Technology of Japan Science and Technology Agency, the Strategic Research Program for Brain Science from MEXT, and the Health Labor Sciences Research Grant on Amyloidosis.

<sup>1</sup> Both authors contributed equally to this work.

<sup>2</sup> To whom correspondence should be addressed: Dept. of Neuropathology, Graduate School of Medicine, University of Tokyo, 7-3-1 Hongo, Bunkyo-ku, Tokyo, 113-0033 Japan. Tel.: 81-3-5841-3541; Fax: 81-3-5841-3613; E-mail: iwatsubo@m.u-tokyo.ac.jp.

<sup>3</sup> The abbreviations used are: AD, Alzheimer disease;  $A\beta$ , amyloid  $\beta$  peptide; FAD, familial AD; APP,  $A\beta$  precursor protein; apoE, apolipoprotein E; ThT, thioflavin T; HFIP, 1,1,1,3,3,3-hexafluoro-2-propanol;  $\alpha 2M$ ,  $\alpha 2$ -macroglobulin; PICUP, photoinduced cross-linking of unmodified protein; SEC, size exclusion chromatography; LMW, low molecular weight; rec, recombinant.

## Roles of ApoE in $\beta$ -Amyloidogenesis *In Vitro* and *In Vivo*

have been reported (15–19). A $\beta$  protofibrils, separated in the high molecular weight fraction (>200 kDa) by size exclusion chromatography (SEC), are flexible short fibrils of ~5 nm in diameter and in lengths not exceeding ~150 nm (15). Because an intra-A $\beta$  E22G (Arctic) FAD mutation accelerates the A $\beta$  protofibril formation (20, 21) and the A $\beta$  protofibrils are shown to be potentially neurotoxic (22, 23), A $\beta$  protofibrils have been deemed as a causative species leading to neurodegeneration in AD brains. However, it remains unclear how A $\beta$  protofibrils impact the pathogenesis of AD.

In this study, we found that intrabrain injection of A $\beta$  protofibrils promoted A $\beta$  deposition in APP transgenic mice, demonstrating that A $\beta$  protofibrils act as aggregation seeds in brains *in vivo*. We further showed that injection of mixture of A $\beta$  protofibrils and apoE3 attenuated A $\beta$  deposition compared with A $\beta$  protofibrils alone or with mixture of A $\beta$  protofibrils and apoE4. Based on these data, we hypothesized that apoE affects A $\beta$  fibrillization, especially during the process of conversion from protofibrils to fibrils, in an isoform-dependent manner. To test this hypothesis, we carried out *in vitro* experiments using SEC analysis and thioflavin T (ThT) binding assay (21) and showed that apoE2 or apoE3 induced the slower conversion of A $\beta$  protofibrils to fibrils than apoE4. We also found that A $\beta$  protofibril-apoE2 or -apoE3 complex was more stable than A $\beta$  protofibril-apoE4 complex. These results support the notion that apoE2 or apoE3 inhibits A $\beta$  fibrillization and attenuates A $\beta$  deposition through suppression of the conversion of A $\beta$  protofibrils to fibrils, whereas apoE4 had a weaker effect.

### Experimental Procedures

**Peptide and Reagents**—Synthetic A $\beta$ (1–42) peptides were purchased from Peptide Institute, Inc.. Peptides were solubilized in 1,1,1,3,3,3-hexafluoro-2-propanol (HFIP; Kanto Chemical) at a concentration of 1 mg/ml, dried, resolubilized in PBS containing 2% (v/v) DMSO (Kanto Chemical) and filtrated through a 0.2- $\mu$ m filter immediately prior to use, as described (21). Human recombinant apoE (Wako Pure Chemical), human  $\alpha$ 1-microglobulin (Dako), and human  $\alpha$ 2-macroglobulin ( $\alpha$ 2M)(Sigma) proteins were purchased from indicated vendors. Lipidated apoE particles were purified from culture media of immortalized astrocytes overexpressing human apoE3 or apoE4 using an affinity column as described (24). Briefly, astrocytes were cultured in advanced DMEM (Life Technologies) with 10% FBS. After reaching at 80–90% confluency, cells were washed by PBS and further incubated in advanced DMEM with N-2 supplement (Life Technologies) and 3  $\mu$ M of 25-hydroxycholesterol (Sigma) during days 2 and 3. Collected culture media were applied onto a column conjugated with a mouse monoclonal antibody against human apoE (WUE-4). Lipid apoE particles were eluted from the column with 3 M sodium thiocyanate, concentrated using Apollo centrifugal quantitative concentrators (QMWL: 150 kDa, Orbital Biosciences) and dialyzed against PBS containing 0.02% sodium azide.

**Animals**—A7 mice are transgenic mice that overexpress human APP695 harboring K670N, M671L, and T714I FAD mutations in neurons under the control of Thy1.2 promoter (25). C57Bl/6N mice were used as wild-type animals. All animals were maintained on food and water with a 12-h light/dark

cycle. All experiments were approved by the Institutional Animal Care and Use Committee of the Graduate School of Pharmaceutical Sciences of the University of Tokyo.

***In Vivo* A $\beta$  Seeding Assay**—*In vivo* A $\beta$  seeding assays were carried out as previously described (26). Briefly, 0.25  $\mu$ g of low molecular weight (LMW) soluble A $\beta$  (22  $\mu$ M A $\beta$ (1–42) without incubation), A $\beta$  protofibril without apoE (22  $\mu$ M A $\beta$ (1–42) with incubation at 37 °C for 3 h), A $\beta$  fibril (22  $\mu$ M A $\beta$ (1–42) after incubation at 37 °C for 24 h), A $\beta$  protofibril with apoE3 or apoE4 (22  $\mu$ M A $\beta$ (1–42), and 220 nM apoE after incubation at 37 °C for 3 h) or PBS were injected into the hippocampus (anterior-posterior –2.5 mm, medial-lateral  $\pm$ 2.0 mm, dorsal-ventral –1.8 mm from Bregma) and the cortex (anterior-posterior –2.5 mm, medial-lateral  $\pm$ 2.0 mm, dorsal-ventral –1.0 mm from Bregma) in 8- or 12-month-old A7 and wt mice, respectively. At 4 months after injection, immunohistochemical staining for A $\beta$  and the measurement of insoluble A $\beta$  were carried out. For A $\beta$  immunohistochemistry, paraffin-embedded sections of mouse brains were pretreated with microwave (550 W, 10 min) in citrate buffer (pH 6.0) followed by proteinase K treatment (100  $\mu$ g/ml, 6 min) and then immunostained with an anti-A $\beta$  mouse monoclonal antibody 82E1 (IBL) by avidin-biotin complex method using diaminobenzidine as chromogen. To biochemically quantitate the insoluble A $\beta$ , the hippocampus of the injected side was extracted by stepwise homogenization by radioimmune precipitation assay buffer (50 mM of Tris-HCl, pH 7.4, 150 mM of NaCl, 1% of Nonidet P-40, 1% of sodium deoxycholate, 0.1% of SDS) buffer containing Complete protease inhibitor mixture (Roche), 2% SDS, and 70% formic acid. The levels of A $\beta$  in formic acid fractions (insoluble A $\beta$ ) were measured by two-site ELISA. The ratio representing the increase in A $\beta$  deposition was calculated as follows:  $\{A7(A\beta) - A7(PBS)\} - \{wt(A\beta) - wt(PBS)\}/A7(PBS)$ , where A7(A $\beta$ ) is insoluble A $\beta$ 42 in the hippocampus of A7 mice injected with A $\beta$ ; A7(PBS) is insoluble A $\beta$ 42 in the hippocampus of A7 mice injected with PBS (*i.e.* contralateral side of A $\beta$  injection); wt(A $\beta$ ) is insoluble A $\beta$ 42 in the hippocampus of wt mice injected with A $\beta$ ; and wt(PBS) is insoluble A $\beta$ 42 in the hippocampus of wt mice injected with PBS (*i.e.* contralateral side of A $\beta$  injection).

In experiments comparing A $\beta$  protofibril injection without apoE and with apoE3 or apoE4, the ratios of the levels of insoluble A $\beta$ 42 in the hippocampus injected with protofibril A $\beta$  and apoE divided by those without apoE were calculated. In experiments comparing the effects of apoE3 and apoE4, the ratios of the levels of insoluble A $\beta$ 42 in the hippocampus injected with A $\beta$  protofibrils with apoE4 divided by those with apoE3 were calculated.

***In Vitro* Assays for the Formation of A $\beta$  Protofibrils and Fibrils**—*In vitro* A $\beta$  fibrillization assays were performed as previously described (21). Briefly, synthetic A $\beta$ (1–42) was solubilized at a concentration of 22  $\mu$ M without or in the presence of indicated proteins (apoE,  $\alpha$ 1-microglobulin, or  $\alpha$ 2M) at a concentration of 220 nM and incubated at 37 °C. Following incubation for the indicated times, 50- $\mu$ l aliquots were put immediately on ice to prevent further fibril formation and were centrifuged at 17,000  $\times$  g for 5 min. After centrifugation, samples before and after centrifugation (total ThT and sup ThT, respectively) were mixed with 500  $\mu$ l of 3  $\mu$ M ThT (Tokyo

Chemical) in 0.1 M glycine-NaOH (pH 8.5) to monitor fibril formation. Fluorescence levels were then assayed using a Hitachi F2500 fluorometer ( $\lambda_{\text{ex}} = 443$  nm and  $\lambda_{\text{em}} = 484$  nm). The supernatants were fractionated by SEC on Superdex 75 column (GE Healthcare Bio-Sciences) attached to a series 1100 high performance liquid chromatograph (Hewlett-Packard) at a flow rate of 0.5 ml/min to monitor protofibril formation at room temperature. A $\beta$  protofibrils and LMW A $\beta$  were detected at elution times of  $\sim 15$  and  $\sim 27$  min, respectively, by UV absorbance at 214 nm. The start time of A $\beta$  fibrillization was defined as the point when the difference of ThT binding between sample prior to and after centrifugation exceeds 1.0.

**Negative Stain Electron Microscopy**—Samples were spread on 400-mesh collodion-coated grids, negatively stained with 2% (w/v) phosphotungstic acid (pH 7.0; Wako Pure Chemical), and viewed in an electron microscope (JEOL 1200EXII), as described (21).

**Immunoblot Analysis**—SDS-PAGE was performed as previously described (21). Samples were loaded on 10–20% Tris-Tricine gradient gels (Cosmo Bio), and A $\beta$  was detected by a mouse monoclonal antibody BAN50, as described (27). ApoE was detected by a mouse monoclonal antibody 3H1 (University of Ottawa Heart Institute Research Corporation) or a goat polyclonal antibody 11-S (Alpha Diagnostic Intl. Inc.).  $\alpha 1$ -Microglobulin was detected by a rabbit monoclonal anti- $\alpha 1$ -microglobulin-specific antibody (Abcam).  $\alpha 2\text{M}$  was detected by a rabbit polyclonal anti- $\alpha 2\text{M}$ -specific antibody (Dako).

**Photoinduced Cross-linking of Unmodified Proteins (PICUP)**—To examine the binding of A $\beta$  and apoE, the PICUP method was applied, as previously described (16). Briefly, 22  $\mu\text{M}$  A $\beta$ (1–42) was incubated without or with apoE at 37 °C for the indicated times, and 1  $\mu\text{l}$  of 1 mM Ru(Bpy) and 1  $\mu\text{l}$  of 20 mM ammonium persulfate (Kanto Chemical) were added to 18  $\mu\text{l}$  of A $\beta$  samples. The mixture was irradiated exactly for 1 s, and the reaction was quenched immediately with 20  $\mu\text{l}$  of 2 $\times$  sample buffer containing 5%  $\beta$ -mercaptoethanol. Then the solution was subjected to immunoblot analysis.

**Protofibril Stability Assay**—Isolated A $\beta$  protofibrils without or with apoE by SEC analysis was incubated at 37 °C for the indicated times. After incubation, the solution was centrifuged, followed by ThT binding assay of the total solution and the supernatants to evaluate the amount of A $\beta$  protofibrils and fibrils.

**Stability Assay for the SDS-stable A $\beta$ -apoE Complex**—To monitor the stability of SDS-stable A $\beta$ -apoE complexes, A $\beta$ (1–42) was incubated with apoE at 37 °C for 6 h, followed by the addition of urea (Nacalai Tesque) or HFIP (Kanto Chemical) at the indicated concentrations and incubated at 4 °C for 12 h. The solution was then subjected to immunoblot analysis.

**Statistical Analysis**—Statistical significance was determined by Student's *t* test for comparison of two groups or by one-way analysis of variance followed by a Tukey-Kramer post hoc test for multiple comparisons tests for comparison of more than two groups. The significance level was established at  $p < 0.05$ . The values are expressed as means  $\pm$  S.D. or S.E.D.

## Results

**A $\beta$  Protofibrils Exhibit a Seeding Effect on A $\beta$  Deposition in the Brains of APP Transgenic Mice**—In this study, we used APP transgenic mice (A7 line), which overexpress human APP with

Swedish and Austrian double FAD-linked mutations (KM670/671NL + T714I) in neurons under the control of Thy1.2 promoter (25). A7 mice develop progressive A $\beta$  deposition in the cerebral neocortices and hippocampi at the age of  $\sim 11$ –12 months in an age-dependent manner.

It has been reported that intracerebral inoculation of A $\beta$  amyloid induces A $\beta$  deposition in the brains of APP transgenic mice, acting as an aggregation seed for A $\beta$  amyloid (26, 28). To elucidate whether A $\beta$  protofibrils also work as an aggregation seed for A $\beta$  amyloid *in vivo*, we prepared LMW A $\beta$ , A $\beta$  protofibrils, and A $\beta$  fibrils using synthetic human A $\beta$ (1–42) (21) and injected them individually into the brains of 8-month-old A7 or wt mice (Fig. 1A). We also injected PBS into the contralateral hemisphere as a control. After 4 months, immunohistochemical analyses of the brains of A7 mice showed that A $\beta$  protofibrils and A $\beta$  fibrils, but not LMW A $\beta$ , induced A $\beta$  deposition around the injection sites (Fig. 1B). In sharp contrast, no A $\beta$  deposits were seen in the PBS-injected contralateral hemisphere (Fig. 1B) or in both hemispheres of wt mice (Fig. 1C). The levels of insoluble A $\beta$  in the brains injected with A $\beta$  protofibrils were significantly higher than those with LMW A $\beta$ , and those in mice injected with A $\beta$  fibrils were higher compared with those injected with A $\beta$  protofibrils, as quantified by A $\beta$  specific ELISA (Fig. 1D). These data suggested that not only A $\beta$  fibrils but also A $\beta$  protofibrils harbor a seeding potential on A $\beta$  amyloidogenesis *in vivo*.

**ApoE3, but Not ApoE4, Attenuates A $\beta$  Deposition Induced by A $\beta$  Protofibrils**—We hypothesized that apoE may affect the seeding effects of A $\beta$  protofibrils in an isoform-dependent manner. To test this, we injected A $\beta$  protofibrils alone into one side of the hippocampus of 12-month-old A7 mice and A $\beta$  protofibrils with apoE3 or apoE4 into the other side (Fig. 2A). We found that A $\beta$  protofibrils with apoE3 induced significantly less abundant A $\beta$  deposition as revealed by immunohistochemistry (Fig. 2B) or as the amount of biochemically extractable insoluble A $\beta$  compared with those injected with A $\beta$  protofibrils alone (Fig. 2C). In contrast, A $\beta$  protofibrils with apoE4 induced A $\beta$  deposition at a similar extent to A $\beta$  protofibrils alone (Fig. 2D). No significant difference in the amount of insoluble A $\beta$  was seen between mice injected with A $\beta$  protofibrils with apoE4 or A $\beta$  protofibrils alone (Fig. 2E). We speculated that these contrasting results were due to the difference between the isoforms of injected apoE. To examine this idea, we injected A $\beta$  protofibrils with apoE3 into one side, and A $\beta$  protofibrils with apoE4 into the other side of the hippocampus of 12-month-old A7 mice and found that A $\beta$  protofibrils with apoE4 induced higher levels of A $\beta$  deposition as detected by immunohistochemistry and as insoluble A $\beta$  by biochemistry compared with A $\beta$  protofibrils with apoE3 (Fig. 2, F and G). These data indicated that apoE3, but not apoE4, attenuated A $\beta$  deposition induced by A $\beta$  protofibrils, suggesting that apoE may affect the seeding effect of A $\beta$  protofibrils in an isoform-dependent manner.

**ApoE Suppresses the Protofibril to Fibril Conversion of A $\beta$  in an Isoform-dependent Manner *In Vitro***—To elucidate the mechanism whereby apoE affects the seeding effects of A $\beta$  protofibrils in an isoform-dependent manner, we investigated the role of apoE in the formation of A $\beta$  protofibrils and fibrils *in*

## Roles of ApoE in $\beta$ -Amyloidogenesis *In Vitro* and *In Vivo*

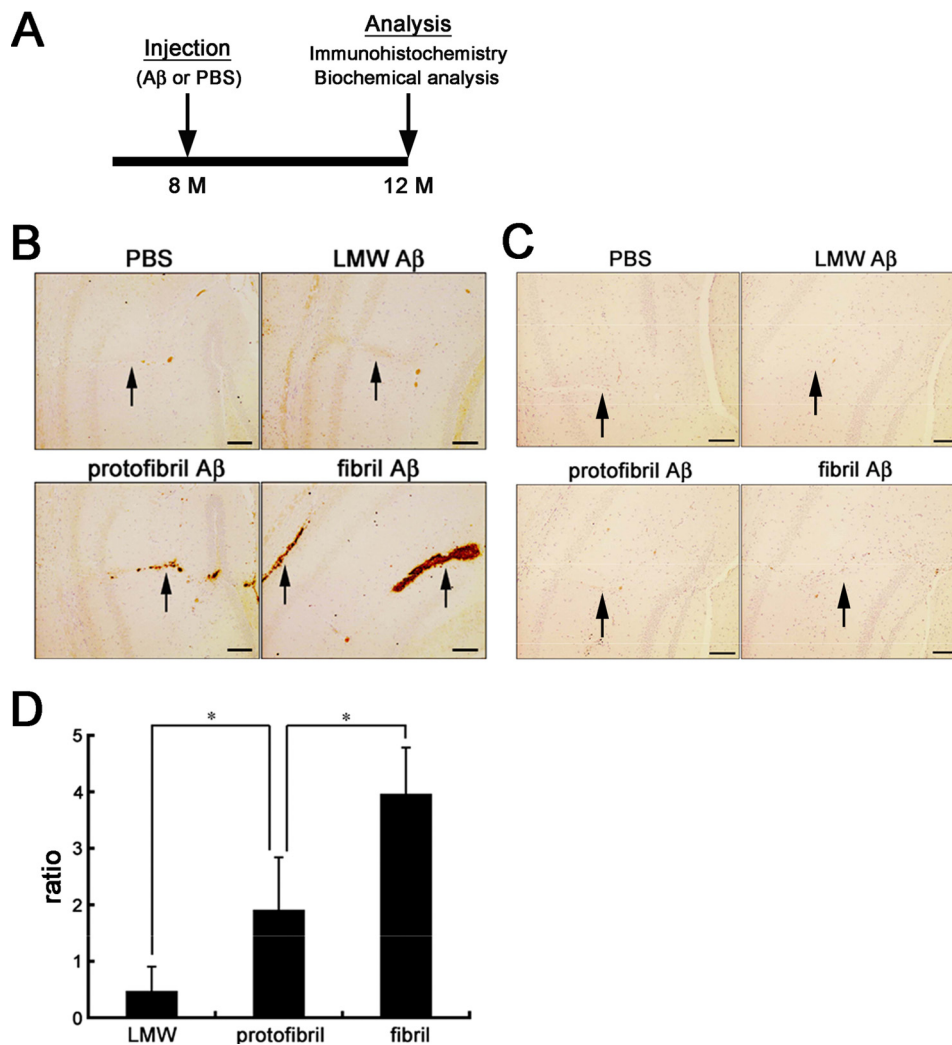


**FIGURE 1. *In vivo* seeding effects of A $\beta$  protofibrils and fibrils in the brains of A7 mice.** *A*, schematic representation of the timeline of experiments. A7 mice were injected with A $\beta$  or PBS into the neocortex and hippocampus at 8 months. Then at 4 months after injection, the both hemispheres were immunohistochemically or biochemically analyzed. *B* and *C*, A $\beta$  immunostaining of the hippocampi and neocortices of mouse brains injected with PBS, LMW, protofibril, or fibril A $\beta$ . A7 mice (*B*) or wt (*C*) mice were injected with PBS, LMW, protofibril, or fibril A $\beta$ , respectively, into the hippocampi and neocortices at 8 months old, and A $\beta$  deposits around the trajectories of injection (arrows) were immunostained by 82E1 at 12 months. Representative images in each group ( $n = 4$ ) are shown. Scale bar, 100  $\mu$ m. *D*, relative levels of insoluble A $\beta$ 42 in the hippocampi of A7 mice injected with different A $\beta$  preparations. Hippocampi of A7 mice injected with PBS, LMW, protofibril, or fibril A $\beta$ , respectively, at 8 months old were dissected at 12 months, and the levels of insoluble A $\beta$ 42 were measured by two-site ELISA. The bars represent the mean ratios of the levels of insoluble A $\beta$ 42 after injection of LMW ( $n = 4$ ), protofibril ( $n = 3$ ), or fibril ( $n = 3$ ) forms of A $\beta$  divided by those injected with PBS. The mean values  $\pm$  S.D. are shown. \*,  $p < 0.05$ . One-way analysis of variance was used.

*in vitro* by SEC analysis and ThT binding assay, respectively, as previously reported (21) (Fig. 3A). Briefly, the formation of A $\beta$  protofibrils and LMW A $\beta$  including monomer and low<sub>n</sub> oligomers, were quantitated as areas corresponding to the >100-kDa peak and the ~10-kDa peak, respectively, detected by SEC analysis. Simultaneously, the formation of A $\beta$  fibrils was evaluated as the difference of ThT binding between samples prior to and after centrifugation (total ThT and sup ThT, respectively). We defined the start time of A $\beta$  fibril formation as the point when the difference of ThT binding between samples prior to and after centrifugation exceeds 1.0. When A $\beta$ (1–42) was incubated, A $\beta$  protofibrils were rapidly formed within 3 h, in parallel with the decrease in LMW A $\beta$ , followed by a decrease in A $\beta$  protofibrils; protofibrils disappeared by 14 h, whereas A $\beta$  fibrils started to increase after 4.6 h of incubation, which leveled off at ~14 h (Fig. 3B). Using these assays, we examined the effect of apoE on the formation of A $\beta$  protofibrils

and fibrils. In comparison with the incubation of A $\beta$  alone (Fig. 3B), coincubation with apoE2 or apoE3 extended the lifetime of A $\beta$  protofibrils and delayed the start of A $\beta$  fibril formation by 7.6 and 13.9 h, respectively (Fig. 3C). In sharp contrast, coincubation with apoE4 did not extend the lifetime of A $\beta$  protofibrils, and fibril formation started at 5.2 h (Fig. 3C). The time course of A $\beta$  fibrillization in the presence of apoE4 was comparable to those in the absence of apoE (Fig. 3B). ApoE is known to be associated with high density lipoprotein particles in the brain and with very low density lipoprotein particles in the blood (29). To see whether lipidation of apoE is critical to the effects on the formation of A $\beta$  protofibrils and fibrils, we used lipidated apoE particles purified from culture media of human immortalized astrocytes overexpressing apoE3 or apoE4 as described (24, 30). We incubated A $\beta$  with or without lipidated apoE particles, monitored the formation of A $\beta$  protofibrils and fibrils, and found that the presence of lipidated apoE particles extended the

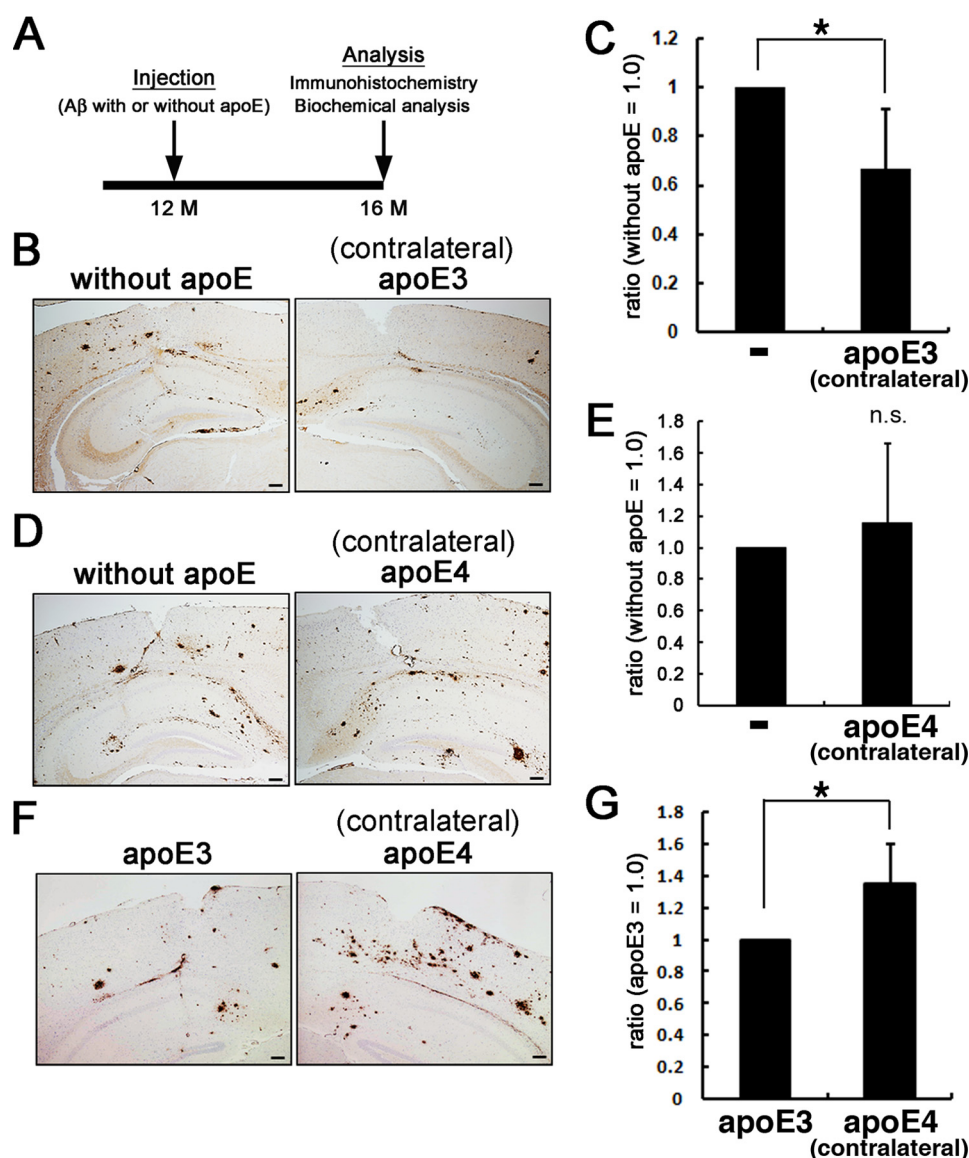


FIGURE 2. *In vivo* effects of apoE on the seeding effects of A $\beta$  protofibrils. *A*, schematic representation of the timeline of experiments. A7 mice were injected with A $\beta$  protofibrils preincubated with or without apoE into the neocortex and hippocampus at 12 months. At 4 months after injection, both hemispheres were immunohistochemically or biochemically analyzed. *B* and *C*, A7 mice were injected with A $\beta$  protofibrils preincubated without apoE on one side of the neocortex and hippocampus and those with apoE3 on the contralateral side. The both hemispheres were immunohistochemically analyzed for A $\beta$  using 82E1 antibody (*B*;  $n = 3$  in each group) or subjected to biochemical quantification of insoluble A $\beta$  (*C*;  $n = 5$ ). Insoluble A $\beta$  levels were quantitated by two-site ELISA, and the ratios of those in the contralateral side (*i.e.* injected with protofibrils preincubated with apoE3) divided by those in the side injected with A $\beta$  protofibrils alone) were calculated (*C*). Similarly, those injected with protofibrils preincubated without apoE on one side and with apoE4 on the contralateral side (*D*;  $n = 3$  in each group, *E*;  $n = 5$ ) and those injected with protofibrils preincubated with apoE3 on one side and with apoE4 on the contralateral side (*F*;  $n = 3$  in each group, *G*;  $n = 5$ ) were immunohistochemically and biochemically analyzed. Scale bars, 100  $\mu$ m. The mean values  $\pm$  S.D. are shown. \*,  $p < 0.05$ .

lifetime of A $\beta$  protofibrils (Fig. 3D); notably, the capacity of lipidated apoE4 particles to prolong the lifetime of A $\beta$  protofibrils was smaller than that of lipidated apoE3 (>24 h in apoE3 versus 14.3 h in apoE4; Fig. 3D). To determine whether apoE altered the structure of protofibrils or fibrils of A $\beta$ , we observed the ultrastructure of A $\beta$  protofibrils or fibrils by negative stain electron microscopy. A $\beta$  protofibrils presented with a short and curved fibril-like structure and A $\beta$  fibrils exhibited a long, straight, and unbranching structure as described (15), which were almost identical between samples of A $\beta$  protofibrils and fibrils in the presence or absence of apoE3 (Fig. 3E). These data suggested that apoE2 and apoE3 potentially suppress the conversion of A $\beta$  protofibrils to fibrils, resulting in the prolonga-

tion of the lifetime of A $\beta$  protofibrils and delay in the start of A $\beta$  fibril formation. In contrast, apoE4 has a lesser effect on the conversion of A $\beta$  protofibrils to fibrils compared with apoE2 or apoE3, thereby allowing A $\beta$  protofibrils with apoE4 to rapidly form fibrils compared with those with apoE2 or apoE3.

*ApoE Forms SDS-stable Complex with A $\beta$  Protofibrils*—Because apoE affected the protofibril to fibril conversion of A $\beta$  in an isoform-dependent manner, we next examined the interaction of apoE with A $\beta$  protofibrils, as well as its isoform dependence. To this end, we coincubated A $\beta$  with different isoforms of apoE *in vitro* and evaluated their interaction by immunoblotting. It has been reported that apoE forms an SDS-stable complex with A $\beta$  (31–33). Upon coincubation of A $\beta$  with apoE2 or

## Roles of ApoE in $\beta$ -Amyloidogenesis *In Vitro* and *In Vivo*

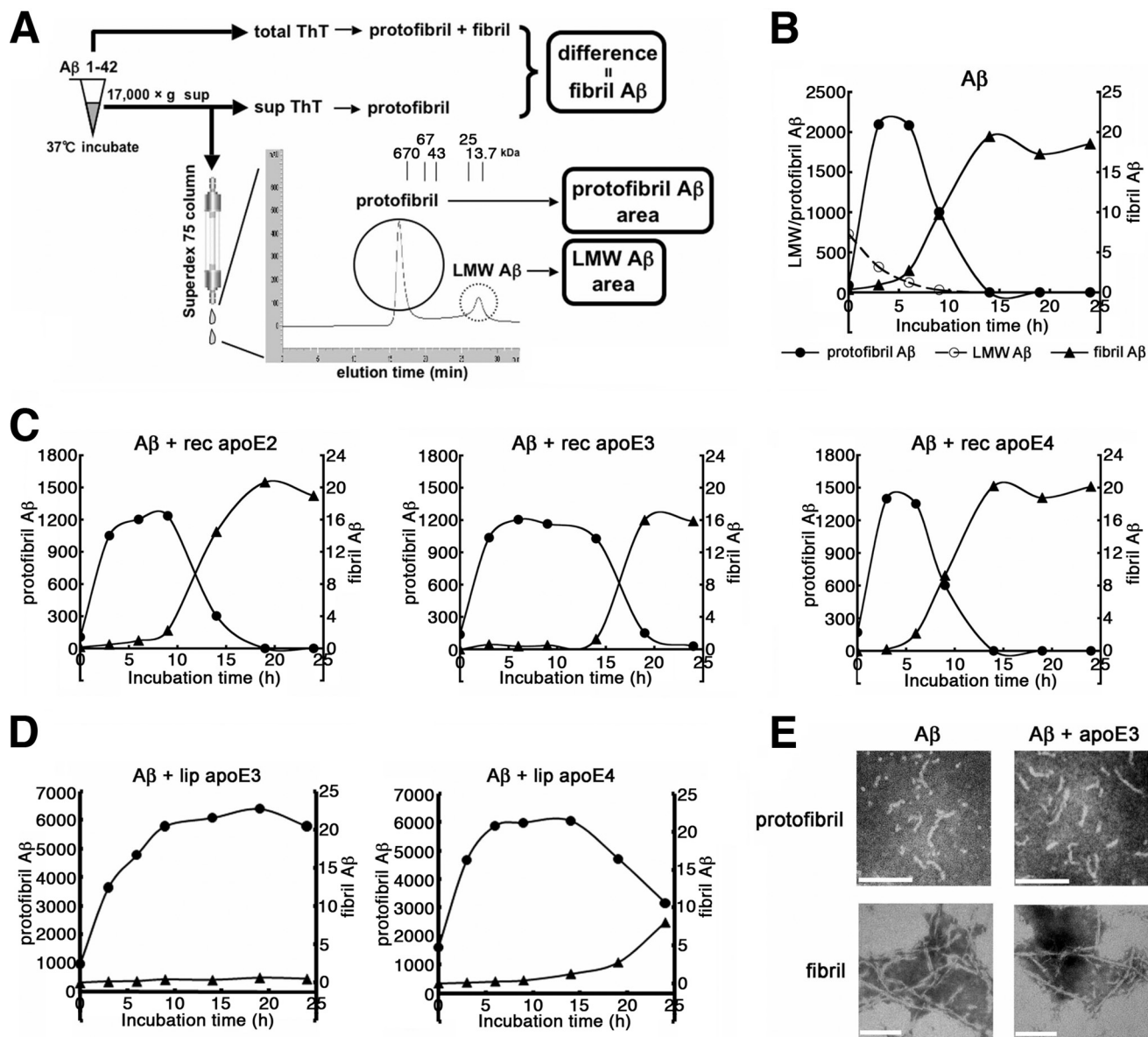


**FIGURE 3. Isoform-dependent effects of apoE on the formation of A $\beta$  protofibrils and fibrils *in vitro*.** *A*, schematic depiction of the method for the measurement of LMW, protofibril, and fibril forms of A $\beta$ . The levels of LMW A $\beta$  and protofibril A $\beta$  are quantitated as areas corresponding to the  $\sim$ 10-kDa peak and  $>$ 100-kDa peak, respectively. The levels of A $\beta$  fibrils are evaluated as the differences of ThT binding between samples prior to (total ThT) and after centrifugation (sup ThT). *B*, time course of the formation of LMW, protofibril, and fibril A $\beta$  as monitored by SEC and ThT binding. 22  $\mu$ M of A $\beta$ (1–42) was incubated for 0, 3, 6, 9, 14, 19, or 24 h, and the levels of LMW A $\beta$  (open circles) and protofibril A $\beta$  (filled circles) were quantitatively evaluated by SEC and those of A $\beta$  fibrils (triangles) by ThT binding, respectively. Representative data out of four independent experiments (that showed similar profiles) are shown. *C*, the effects of recombinant (rec) apoE on the formation of protofibril and fibril A $\beta$ . 22  $\mu$ M of A $\beta$ (1–42) was incubated for 0, 3, 6, 9, 14, 19, or 24 h with 220 nM of rec apoE2 (left panel,  $n = 4$ ), rec apoE3 (middle panel,  $n = 5$ ), or rec apoE4 (right panel,  $n = 4$ ), and the time course of the formation of A $\beta$  protofibrils (circles) and fibrils (triangles) was monitored as in *B*. The starting time points of fibril formation were estimated to be 7.6, 13.9, and 5.2 h, respectively, in preparations incubated with rec apoE2, apoE3, and apoE4. The mean values are shown. *D*, the effects of the lipidated (lip) apoE particles on the formation of protofibril and fibril A $\beta$ . 22  $\mu$ M of A $\beta$ (1–42) was incubated for 0, 3, 6, 9, 14, 19, or 24 h with 220 nM of lipid apoE3 particles (left panel,  $n = 4$ ) or lipid apoE4 particles (right panel,  $n = 4$ ), and the time course of the formation of protofibrils (circles) and fibrils (triangles) were monitored as in *C*. Fibril formation was observed starting at  $>$ 24 h and 24 h of incubation, respectively, in preparations incubated with lipidated (lip) apoE3 and apoE4. The mean values are shown. *E*, negative stain electron micrograph of protofibril and fibril forms of A $\beta$ (1–42) incubated alone (left column) or with apoE3 (right column) for 6 h (protofibrils, upper row) and 24 h (fibrils, lower row), respectively. Scale bar, 100 nm.

apoE3, an anti-A $\beta$  antibody (BAN50) revealed  $\sim$ 40-kDa bands in addition to the A $\beta$  monomer and oligomer bands (Fig. 4, *A* and *B*, upper panels). The  $\sim$ 40-kDa bands were also labeled with an anti-apoE antibody (3H1) (Fig. 4, *A* and *B*, lower panels), indicating that the  $\sim$ 40-kDa bands represented the SDS-stable complex of A $\beta$  and apoE2 or apoE3. Intriguingly, the  $\sim$ 40-kDa bands appeared in a time-dependent manner: the  $\sim$ 40-kDa band did not exist at 0 h, which emerged during 3–9 h upon

coincubation with apoE2 or 3–14 h upon coincubation with apoE3, concomitantly with the A $\beta$  protofibril formation (Fig. 3C). After 9 h of coincubation with apoE2 or 14 h of coincubation with apoE3, the  $\sim$ 40-kDa bands disappeared, which coincided with the emergence of A $\beta$  fibrils (Fig. 3C). These findings are consistent with the idea that apoE was precipitated with A $\beta$  fibrils. In contrast, the  $\sim$ 40-kDa bands were present at 3–6 h of incubation when A $\beta$  was coincubated with apoE4 (Fig. 4C). The

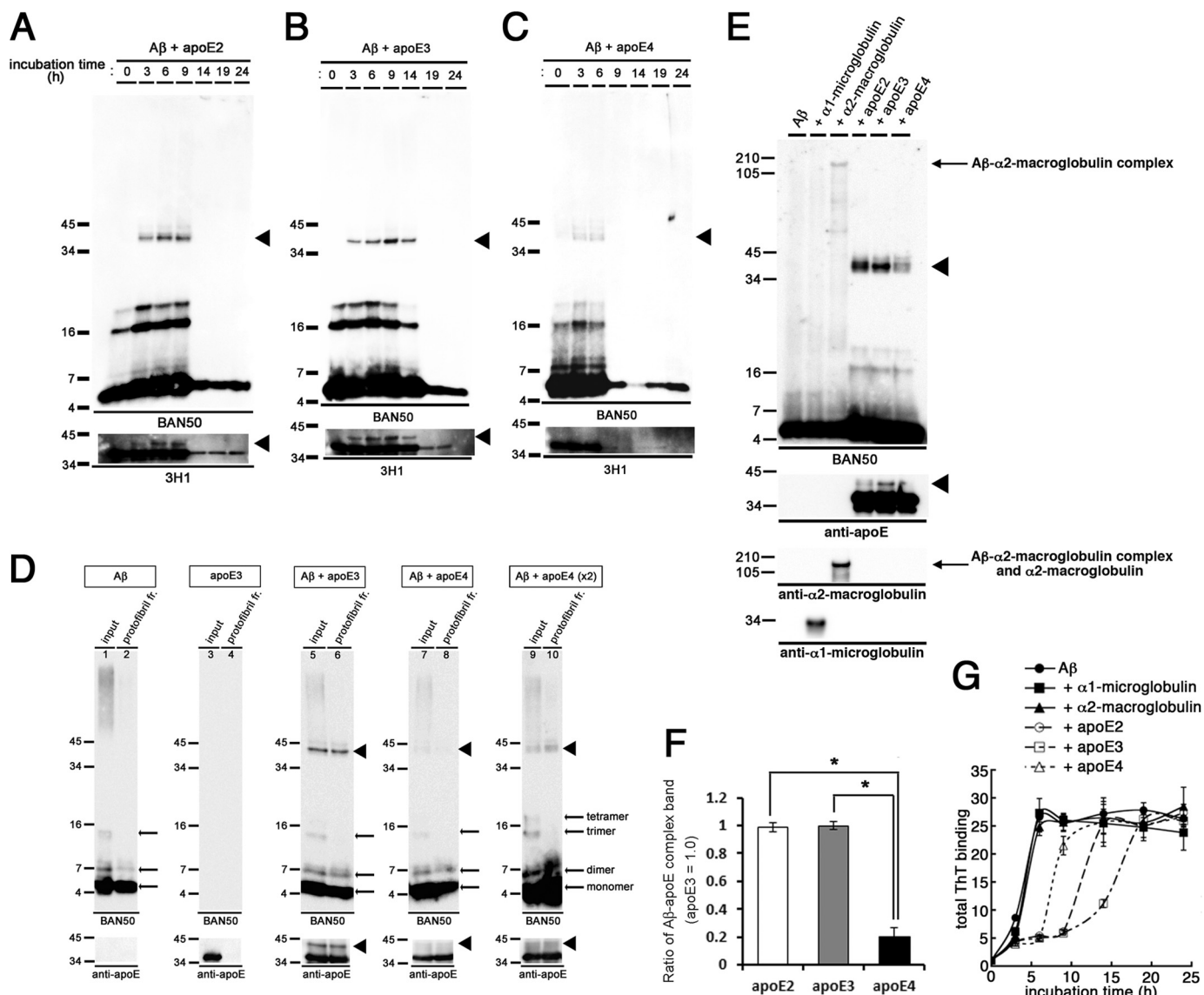


**FIGURE 4. Formation of SDS-stable  $A\beta$ -apoE complex in vitro.** *A–C*, time course of formation of the SDS-stable  $A\beta$ -apoE complex. 22  $\mu$ M of  $A\beta$ (1–42) was incubated for 0, 3, 6, 9, 14, 19, or 24 h with rec apoE2 (*A*), rec apoE3 (*B*), or rec apoE4 (*C*). After centrifugation, SDS-stable  $A\beta$ -apoE complex was monitored by immunoblot analyses with an anti- $A\beta$  antibody (BAN50, upper panel) and an anti-apoE antibody (3H1, bottom panel). Arrowheads indicate the SDS-stable  $A\beta$ -apoE complex bands ( $n = 3$ ). *D*, formation of SDS-stable  $A\beta$ -apoE complex in the  $A\beta$  protofibril fraction. Immunoblot analyses of isolated protofibrils without apoE (lanes 1 and 2), with rec apoE3 (lanes 5 and 6), with rec apoE4 (lanes 7–10), and of rec apoE3 alone (lanes 3 and 4) with an anti- $A\beta$  antibody (BAN50, upper panels) and an anti-apoE antibody (bottom panels). Lanes 9 and 10 were loaded with double the amount of samples. Arrowheads indicate the bands corresponding to SDS-stable  $A\beta$ -apoE complex migrating at  $\sim 40$  kDa ( $n = 3$ ). *E*, 22  $\mu$ M of  $A\beta$ (1–42) was incubated alone ( $A\beta$ ) or with rec  $\alpha$ 1-microglobulin, rec  $\alpha$ 2M, rec apoE2, rec apoE3, or rec apoE4 for 6 h. After centrifugation at  $17,000 \times g$  for 5 min, SDS-stable complex was monitored by immunoblotting analyses using an anti- $A\beta$  antibody (BAN50, upper panel), an anti-apoE antibody (3H1, the second panel from the top), an anti- $\alpha$ 2M antibody (the third panel from the top), and an anti- $\alpha$ 1-microglobulin antibody (bottom panel). Arrowheads indicate  $\sim 40$ -kDa bands corresponding to the SDS-stable  $A\beta$ -apoE complex, and the arrow indicates the SDS-stable  $A\beta$ - $\alpha$ 2M complex migrating at  $\sim 190$  kDa. *F*, quantitative measurement of the band intensities in *E*. The mean values  $\pm$  S.D. in three independent experiments are shown as ratios relative to the values of apoE3 as 1.0. \*,  $p < 0.05$ . One-way analysis of variance was used. *G*, *in vitro*  $A\beta$  fibrillization assay in the presence of binding proteins. 22  $\mu$ M of  $A\beta$ (1–42) was incubated in the absence (filled circles) or presence of rec  $\alpha$ 1-microglobulin (the molar ratio of  $A\beta/\alpha$ 1-microglobulin at 100:1, filled squares), rec  $\alpha$ 2M (the molar ratio of  $A\beta/\alpha$ 2M at 100:1, filled triangles), rec apoE2 (the molar ratio of  $A\beta$ /apoE2 at 100:1, open circles), rec apoE3 (the molar ratio of  $A\beta$ /apoE3 at 100:1, open squares), or rec apoE4 (the molar ratio of  $A\beta$ /apoE4 at 100:1, open triangles) for 0, 3, 6, 9, 14, 19, and 24 h, and then ThT fluorescence was measured. The mean values in three independent experiments are shown.

time course of the emergence of the  $\sim 40$ -kDa bands was coincident with that of  $A\beta$  protofibril formation in the presence of apoE4 (Fig. 3C).

Because the formation of SDS-stable  $A\beta$ -apoE complex coincided with the protofibril formation of  $A\beta$ , we further examined whether apoE was directly bound to  $A\beta$  protofibrils by incubating  $A\beta$  with or without apoE for 6 h and isolating the  $A\beta$  protofibril fraction using SEC. When  $A\beta$  was incubated with-

out apoE,  $A\beta$ -positive bands corresponding to  $A\beta$  monomer and oligomers were detected in the protofibril fraction (Fig. 4D, lane 2), suggesting the dissociation of  $A\beta$  protofibrils during SDS-PAGE into monomer or oligomers. When apoE3 was incubated alone, no apoE-positive band was detected in the  $A\beta$  protofibril fraction (Fig. 4D, lane 4). Importantly, when  $A\beta$  was cocubated with apoE3,  $A\beta$  monomer, oligomers, apoE3, and the  $\sim 40$ -kDa SDS-stable  $A\beta$ -apoE3 complex were detected in

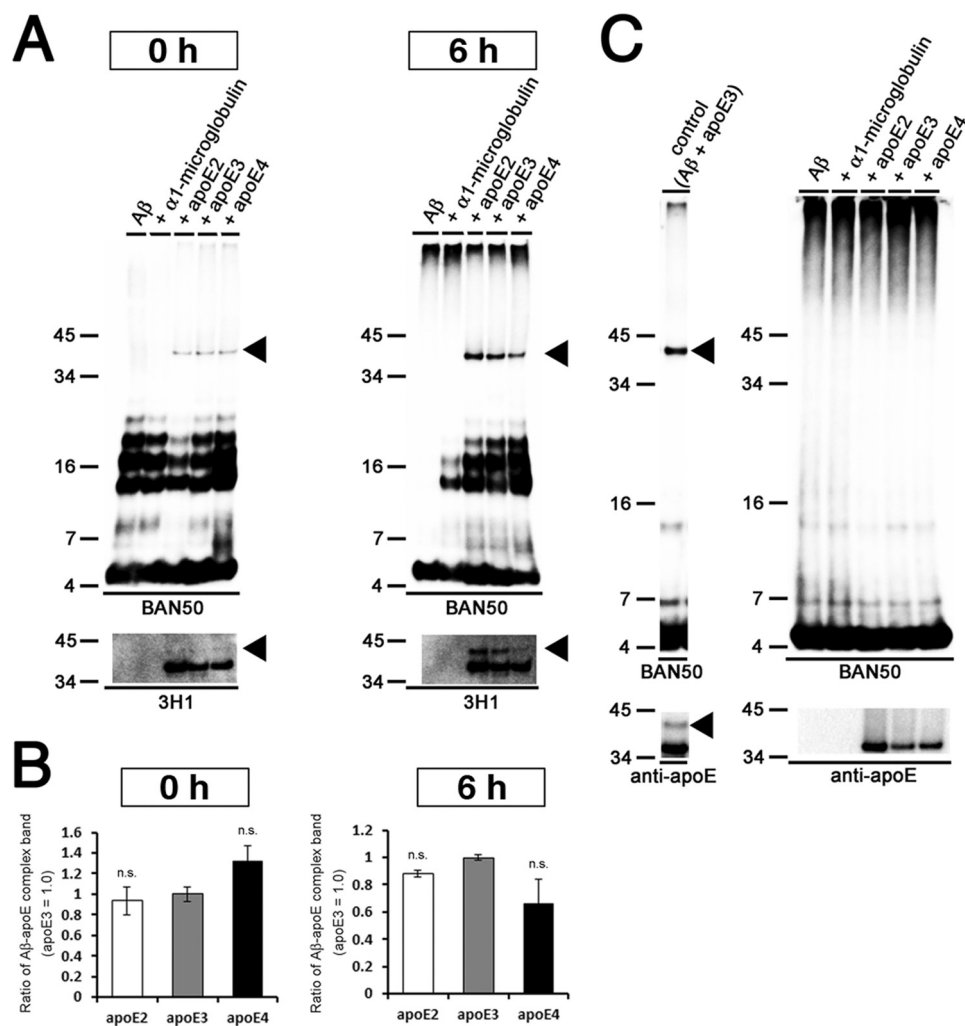


**FIGURE 5. Chemical cross-linking analyses of the interaction between A $\beta$  protofibrils and apoE.** *A*, 22  $\mu$ M of A $\beta$ (1–42) was incubated alone (A $\beta$ ) or with rec  $\alpha$ 1-microglobulin, rec apoE2, rec apoE3, or rec apoE4 for 0 or 6 h and cross-linked by PICUP. The binding between A $\beta$  and apoE was assayed by immunoblot analyses using an anti-A $\beta$  antibody (BAN50, upper panel) and an anti-apoE antibody (3H1, bottom panel). Arrowheads indicate bands corresponding to the SDS-stable A $\beta$ -apoE complex. *B*, quantitative measurement of the band intensities in *A*. The mean values  $\pm$  S.D. in three independent experiments are shown as ratios relative to the values of apoE3 as 1.0. *n.s.* means no significant difference. One-way analysis of variance was used. *C*, formation of SDS-stable A $\beta$ -apoE complex from the preformed protofibrils. Post lanes, 22  $\mu$ M of A $\beta$ (1–42) was incubated for 6 h to generate protofibrils, and thus formed protofibrils were again incubated alone or with rec  $\alpha$ 1-microglobulin, rec apoE2, rec apoE3, or rec apoE4 for 8 h at 37  $^{\circ}$ C. Control lane, 22  $\mu$ M of A $\beta$ (1–42) was incubated for 6 h with rec apoE3. SDS-stable A $\beta$ -apoE complex was detected by immunoblot analyses with an anti-A $\beta$  antibody (BAN50, upper panels) or an anti-apoE antibody (bottom panels). Arrowheads indicate the bands corresponding to SDS-stable A $\beta$ -apoE complex.

the protofibril fraction (Fig. 4*D*, lane 6), indicating that apoE3 directly interacted with A $\beta$  protofibrils and formed the  $\sim$ 40-kDa SDS-stable complex with A $\beta$  protofibrils. In addition, the  $\sim$ 40-kDa band corresponding to the SDS-stable A $\beta$ -apoE4 complex was also detected in the A $\beta$  protofibril fraction by coincubation of A $\beta$  with apoE4 (Fig. 4*D*, lanes 8 and 10). It is notable that the amount of SDS-stable A $\beta$ -apoE4 complex in the A $\beta$  protofibril fraction was markedly smaller than that of SDS-stable A $\beta$ -apoE2 or A $\beta$ -apoE3 complex (Fig. 4, *D–F*), whereas the levels of A $\beta$  in these fractions were similar. These data suggest that apoE formed a SDS-stable complex with A $\beta$  protofibrils in an isoform-dependent manner. To further ascertain the specificity of apoE in the formation of SDS-stable complex with A $\beta$  protofibrils, we coincubated A $\beta$  with  $\alpha$ 1-microglobulin,  $\alpha$ 2M, recombinant apoE2, apoE3, or apoE4 and examined the level of SDS-stable complex by immunoblotting (Fig. 4*E*). We confirmed that apoE2 formed the  $\sim$ 40-kDa SDS-

stable A $\beta$ -apoE complex at a similar extent to apoE3, whereas apoE4 formed smaller amount of SDS-stable A $\beta$ -apoE complex compared with apoE3 (Fig. 4, *E* and *F*).  $\alpha$ 1-Microglobulin did not form the SDS-stable complex with A $\beta$ , whereas  $\alpha$ 2M, which is capable of binding with A $\beta$ , formed A $\beta$ - $\alpha$ 2M SDS-stable complex as a  $\sim$ 190-kDa band. Because  $\alpha$ 2M did not affect the A $\beta$  fibrillization *in vitro* (Fig. 4*G*), we presumed that the interaction of  $\alpha$ 2M with A $\beta$  did not affect the conversion of A $\beta$  from protofibrils to fibrils.

**A $\beta$  Interacts with apoE Prior to Protofibril Formation**—Since apoE formed the SDS-stable complex with A $\beta$  protofibrils in an isoform-dependent manner, we examined whether the binding affinity of apoE to A $\beta$  differs among apoE isoforms. To examine the interaction between apoE and A $\beta$  in solution, we performed chemical cross-linking assay using the PICUP method (16). We found that all apoE isoforms bound to A $\beta$  at 0 or 6 h with no difference in the levels of the A $\beta$ -apoE complex of  $\sim$ 40 kDa



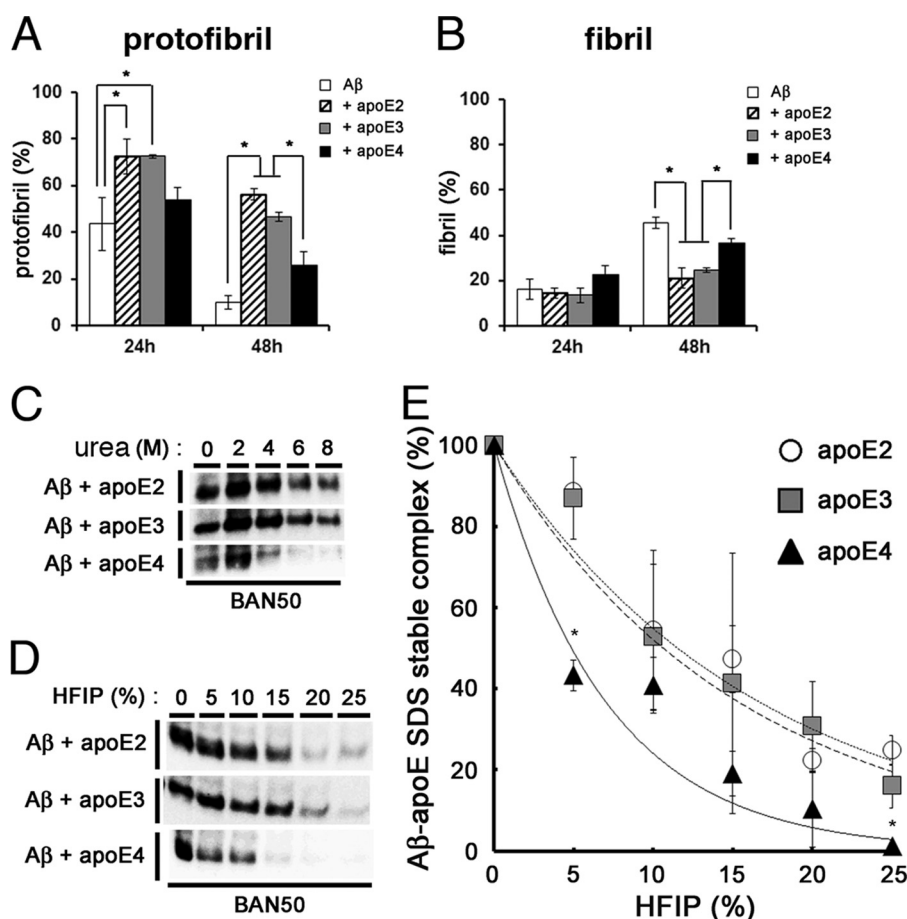


**FIGURE 6. Isoform-dependent effects of apoE on the stability of A $\beta$  protofibrils.** *A* and *B*, the effects of apoE on the stability of A $\beta$  protofibrils (*A*) and formation of fibrils (*B*). A $\beta$  protofibrils isolated by SEC were incubated alone (*white column*), with rec apoE2 (*hatched column*), with rec apoE3 (*gray column*), or rec apoE4 (*black column*) for 24 and 48 h. After centrifugation at  $17,000 \times g$  for 5 min, the levels of protofibrils were monitored by the ThT fluorescence of supernatants, and those of fibrils were determined by the difference in ThT fluorescence between samples before and after centrifugation. The percentage of levels of protofibrils (*A*) and fibrils (*B*) at 24 or 48 h that comprise those prior to incubation as 100% (mean values  $\pm$  S.D. in three independent experiments) are shown. \*,  $p < 0.05$ . One-way analysis of variance was used. *C*, stability of SDS-stable A $\beta$ -apoE complex against urea.  $22 \mu\text{M}$  of A $\beta$ (1–42) was incubated for 6 h with rec apoE2, rec apoE3, or rec apoE4, followed by addition of urea at 0, 2, 4, 6, or 8 M of final concentrations and additionally incubated for 12 h. SDS-stable A $\beta$ -apoE complex was detected by immunoblot analyses with an anti-A $\beta$  antibody (BAN50). *D*, stability of SDS-stable A $\beta$ -apoE complex against HFIP.  $22 \mu\text{M}$  of A $\beta$ (1–42) was incubated for 6 h with rec apoE2, rec apoE3, or rec apoE4, followed by addition of HFIP at 0, 5, 10, 15, 20, or 25% of final concentrations and additionally incubated for 12 h. SDS-stable A $\beta$ -apoE complex was detected by immunoblot analyses with an anti-A $\beta$  antibody (BAN50). *E*, quantitation of data in *D*. The levels of A $\beta$ -apoE2 (*circles*), A $\beta$ -apoE3 (*squares*), and A $\beta$ -apoE4 (*triangles*) complexes after addition of indicated concentrations of HFIP were evaluated by densitometry. The mean values  $\pm$  S.D. in three independent experiments are shown. \*,  $p < 0.05$ . One-way analysis of variance was used.

(Fig. 5, *A* and *B*). To determine whether apoE binds to the preformed A $\beta$  protofibrils, we coincubated preformed A $\beta$  protofibrils with apoE. No bands corresponding to SDS-stable A $\beta$ -apoE complex were detected (Fig. 5*C*), suggesting that apoE initially binds to soluble A $\beta$  and that apoE may form SDS-stable complex with A $\beta$  protofibrils in an isoform-dependent manner during the course of A $\beta$  fibrillization.

**ApoE4 Forms a Less Stable Complex with A $\beta$  Protofibrils Compared with ApoE2 or ApoE3**—It remained unknown why apoE2 or apoE3 suppressed the conversion of A $\beta$  protofibrils to fibrils more efficiently than apoE4 and formed a more SDS-stable complex with A $\beta$  protofibrils than apoE4. We hypothesized that apoE may have a role in stabilizing A $\beta$  protofibrils in an isoform-dependent manner. To test this, we first evaluated the stability of A $\beta$  protofibrils isolated by SEC. We incubated the SEC-isolated A $\beta$  protofibrils at  $37^\circ\text{C}$  for 24 and 48 h, respectively, centrifuged, and monitored the remaining A $\beta$  protofibrils in the supernatants by ThT binding (Fig. 6*A*). We found that  $\sim 56.2\%$  and  $\sim 46.7\%$  of A $\beta$  protofibrils formed in the

presence of apoE2 and apoE3, respectively, remained after 48 h of incubation. In contrast,  $\sim 9.9\%$  and  $\sim 26.0\%$  of A $\beta$  protofibrils formed without apoE or in the presence of apoE4, respectively, persisted after incubation. Simultaneously, we measured the levels of A $\beta$  fibrils, which were formed during the incubation period, by ThT binding assay. The ratios of A $\beta$  fibrils formed from A $\beta$  protofibrils incubated with apoE2 and apoE3 were  $\sim 21.1\%$  and  $\sim 24.7\%$ , respectively, after 48 h of incubation (Fig. 6*B*), whereas those with apoE4 or without apoE were  $\sim 46.0\%$  and  $\sim 36.8\%$ , respectively (Fig. 6*B*). These data strongly suggested that apoE3 had the capacity to stabilize A $\beta$  protofibrils by suppressing the conformational change into fibrils, whereas apoE4 had a weaker effect on the stabilization of A $\beta$  protofibrils.

To further examine the effect of apoE2 or apoE3 on the stability of A $\beta$  protofibrils, we tested the stability of the protofibril A $\beta$ -apoE complex by chemical-induced denaturation. We incubated the SDS-stable A $\beta$ -apoE complex in different concentrations of urea solution (0, 2, 4, 6, or 8 M) and found that complexes of A $\beta$ -apoE2 or A $\beta$ -apoE3 were stable, even in the

## Roles of ApoE in $\beta$ -Amyloidogenesis *In Vitro* and *In Vivo*

presence of 8 M urea, whereas SDS-stable A $\beta$ -apoE4 complex was dissociated in 4, 6, or 8 M of urea solution (Fig. 6C). We also incubated the SDS-stable A $\beta$ -apoE complex in 0, 5, 10, 15, 20, or 25% of HFIP and found that the A $\beta$ -apoE2 or A $\beta$ -apoE3 complex was more stable than the A $\beta$ -apoE4 complex (Fig. 6, D and E). These data also suggested that apoE4 rendered the A $\beta$  protofibrils less stable compared with apoE2 or apoE3. Taken together, we concluded that apoE2 or apoE3 forms a more stable complex with A $\beta$  protofibrils, resulting in the suppression of structural conversion of A $\beta$  protofibrils to fibrils, whereas apoE4 does not have this effect.

### Discussion

In this study, we showed that both A $\beta$  protofibrils and fibrils are capable of inducing A $\beta$  deposition in the brain as an amyloid seed, similarly to A $\beta$  amyloid extracted from the brains of AD patients or APP transgenic mice (26, 28), and that apoE3, but not apoE4, had a suppressive effect on the A $\beta$  deposition induced by A $\beta$  protofibrils. We further showed in *in vitro* A $\beta$  protofibril/fibril formation assays that apoE2 and apoE3 prolonged the lifetime of A $\beta$  protofibrils and suppressed the conversion of A $\beta$  protofibrils to fibrils, whereas apoE4 had a lesser effect on the retention of A $\beta$  protofibrils and failed to inhibit the conversion of A $\beta$  protofibrils to fibrils compared with apoE2 or apoE3. Furthermore, we found that A $\beta$  protofibrils interacted with apoE and formed a SDS-stable complex. Finally we showed that SDS-stable A $\beta$ -apoE4 complex was less stable than those containing apoE2 or apoE3, resulting in the lower level of SDS-stable A $\beta$ -apoE4 complex compared with those with apoE2 or apoE3. These data suggest that apoE2 or apoE3 plays a role in the retention of A $\beta$  protofibrils, thereby suppressing the conversion of A $\beta$  protofibrils to fibrils, whereas apoE4 is incapable of sustaining the lifetime of A $\beta$  protofibrils in a loss of function manner. This view is consistent with the results that apoE3 suppressed A $\beta$  fibril formation *in vitro* and attenuated the protofibril-induced A $\beta$  deposition in the brains of APP transgenic mice, whereas apoE4 did not have these effects. It has been reported that the A $\beta$  burden in the brains of patients with AD is increased with  $\epsilon 4$  allele in a dose-dependent manner (10, 34). Overexpression of human apoE4 in the absence of endogenous murine apoE increased the deposition of fibrillar A $\beta$  in the hippocampus of mice, whereas that of apoE3 did not have this effect (35, 36). Taken together, these data support the notion that apoE4 promotes the amyloid fibril formation through the lack of suppression of conversion of A $\beta$  protofibrils to fibrils.

We coinubated A $\beta$  and apoE *in vitro*, separated the protofibril fraction by SEC (~600-kDa ranges; Fig. 3A), and detected a ~40-kDa SDS-stable band by SDS-PAGE that is positive both for A $\beta$  and apoE on immunoblots (Fig. 4, A–D). We speculated that the ~40-kDa band was derived from a subfraction of A $\beta$  protofibrils-apoE complex and examined their amount or stability in detail, although it remains to be determined whether the characteristics of the SDS-stable A $\beta$ -apoE complex represents those of A $\beta$  protofibrils potentially interacting with apoE, because the SDS-stable A $\beta$ -apoE complex comprised a relatively minor fraction of apoE or A $\beta$  (Fig. 4D). Nonetheless, we have shown that the stabilizing activity of apoE4 on A $\beta$  proto-

fibrils was lower than those of apoE2 or apoE3, underscoring the differential effects of apoE isoforms on the stability of protofibrils (Fig. 6A).

It has been reported that the level of A $\beta$  monomer-apoE4 complex was smaller than that of A $\beta$  monomer-apoE3 complex *in vitro* by immunoblotting (32). Recently, it has also been reported that soluble A $\beta$ -apoE4 complex is less stable than A $\beta$ -apoE2 or A $\beta$ -apoE3 *in vitro* as measured by A $\beta$ -apoE complex-specific ELISA and that the levels of soluble A $\beta$ -apoE complex are lower in 5xFAD-apoE4TR mice compared with those in 5xFAD-apoE3TR or 5xFAD-apoE2TR mice *in vivo* (37). In the present study, we show that the level of SDS-stable A $\beta$ -apoE4 protofibril complex in the A $\beta$  protofibril fraction was lower than that of SDS-stable A $\beta$ -apoE3 protofibril complex. These data suggest an isoform-specific effect of apoE on the stability of the A $\beta$ -apoE complex, *i.e.* A $\beta$ -apoE3 complex being more stable than A $\beta$ -apoE4 complex (38). Furthermore, we show that the stability of A $\beta$  protofibril-apoE4 complex was lower than that of A $\beta$  protofibril-apoE2 or A $\beta$  protofibril-apoE3 complex *in vitro*, suggesting that apoE isoforms differentially stabilize both protofibrils and monomers of A $\beta$ . However, the mechanism of the isoform-specific stabilization of A $\beta$  protofibrils by apoE remains unclear. The A $\beta$  protofibril-apoE4 complex may have a thermodynamically higher energy state compared with A $\beta$  protofibril-apoE2 or apoE3 complexes; this could enable the faster transition of the conformation of A $\beta$  protofibrils with apoE4 into fibrils compared with apoE2 or apoE3, because of the lower activation barrier. It has been documented that apoE4 forms a compact structure by the salt bridge between Arg-61 and Glu-255, whereas apoE2 and apoE3 have an open structure without the salt bridge (39, 40). Moreover, substitution of Thr for Arg-61 in apoE4, which mimics the open structure of apoE3, formed more SDS-stable A $\beta$ -apoE complex than apoE4 (41). These observations support the notion that the difference in the tertiary structure of apoE affects the isoform-dependent differences in the stability of A $\beta$  protofibril-apoE complexes, which may result in affecting the rate of the conformational changes of A $\beta$  protofibrils to fibrils.

Our *in vivo* experiments showed that the injection of A $\beta$  protofibrils into the brain of APP transgenic mice induced A $\beta$  deposition. Our results indicate that A $\beta$  protofibrils are capable of acting as an aggregation seed *in vivo*. This also suggests that the A $\beta$  protofibrils act as “on pathway” intermediates that promote A $\beta$  amyloid formation. A $\beta$  protofibrils have been identified as a toxic, soluble, and fibril-like intermediate in an *in vitro* A $\beta$  fibrillization assay (22, 23). It has been reported that A $\beta$  protofibrils were detected in the brain and cerebrospinal fluid of APP transgenic mice using an antibody specific for A $\beta$  protofibrils (42) and that passive immunization with the A $\beta$  protofibril-specific antibody significantly reduced the amyloid burden in the brains of APP transgenic mice (43). In addition, it has been reported that E22G (Arctic) FAD mutation that alters an amino acid residue within A $\beta$  region accelerates protofibril formation *in vitro* (20), as well as amyloid deposition in the brains of APP transgenic mice (44). These data suggest that A $\beta$  protofibrils play critical roles in A $\beta$  fibrillization and in A $\beta$  amyloid deposition in the brains of AD patients as an aggregation seed. Furthermore, we showed that apoE3, but not apoE4, attenuated

the A $\beta$  deposition induced by inoculation of A $\beta$  protofibrils into the brains of APP transgenic mice. These results suggest that apoE affects the seeding effect of A $\beta$  protofibrils in an isoform-dependent manner.

In the *in vitro* protofibril/fibril formation study, the lifetime of A $\beta$  protofibrils coincubated with apoE4 was shorter than that of protofibrils with apoE2 or apoE3. This apparently contradicts with the finding that the FAD-linked E22G (Arctic) mutation increases the level of A $\beta$  protofibrils (20). The discrepancy may partly be explained by the limited amount of A $\beta$  peptides within the reaction tube in the *in vitro* experimental setting, resulting in the monophasic emergence of A $\beta$  protofibrils and subsequent conversion to fibrils. In human brains *in vivo*, A $\beta$  is continuously produced and supplied to the brain parenchyma; once A $\beta$  starts to aggregate in the brain, we postulate that the level of protofibrils is maintained at a plateau, at an equilibrium between formation of A $\beta$  protofibrils and structural conversion to fibrils, resulting in an increase in the level of A $\beta$  deposition in the brain, without reducing the level of pathogenic A $\beta$  protofibrils. We have previously reported that H6R (English) and D7N (Tottori) FAD-linked mutations accelerated A $\beta$  fibril formation without an increase in the protofibril formation *in vitro* (21), suggesting that the acceleration of structural conversion of A $\beta$  protofibrils to fibrils may be a mechanism causative for AD. Recently, it has been reported that apoE4 increases the formation of soluble A $\beta$  oligomers more markedly than apoE2 or apoE3 in the brains of AD patients (30, 37). Taken together, it is conceivable that the entire process of A $\beta$  fibrillization is suppressed by apoE2 or apoE3, thereby causing the attenuation of amyloid deposition in the brain, whereas apoE4 does not have these effects, thereby causing the enhanced amyloid deposition phenotype observed in APOE4 carriers in AD. It also remains possible that A $\beta$  protofibrils complexed with apoE4 have a higher neuronal toxicity compared with those with apoE2 or apoE3.

In present study, we specifically investigated the effects of apoE on the process of A $\beta$  fibrillization and deposition. Recent studies also highlight the roles of apoE in the metabolism and clearance of A $\beta$  in the brain (45). Using an *in vivo* microdialysis technique, it is reported that apoE-null mice, in which reduced A $\beta$  deposition has been documented (46), had a significantly shorter half-life of soluble A $\beta$  in the brain interstitial fluids (47). These data suggest that the effects of apoE on the metabolism and clearance of A $\beta$  should also be taken into account in the understanding of A $\beta$  economy in brains.

In summary, we show that apoE is involved in the process of A $\beta$  fibrillization and A $\beta$  deposition in an isoform-dependent manner: apoE2 or apoE3 suppresses the conversion of A $\beta$  protofibrils to fibrils and attenuates A $\beta$  deposition, whereas apoE4 is incapable of suppressing the conversion, presumably by the lack of a stabilizing activity. These findings add to our understanding as to why APOE  $\epsilon$ 4 allele is a major risk factor for AD and support the idea that regulating the interaction between A $\beta$  and apoE may be a promising therapeutic target for the inhibition of fibrillization and deposition of A $\beta$  in the brain.

*Acknowledgments*—We thank Dr. T. Wakabayashi and other lab members for helpful discussions.

## References

- Selkoe, D. J. (2001) Alzheimer's disease: genes, proteins, and therapy. *Physiol. Rev.* **81**, 741–766
- Dickson, D. W. (1997) The pathogenesis of senile plaques. *J. Neuropathol. Exp. Neurol.* **56**, 321–339
- Boyles, J. K., Pitas, R. E., Wilson, E., Mahley, R. W., and Taylor, J. M. (1985) Apolipoprotein E associated with astrocytic glia of the central nervous system and with nonmyelinating glia of the peripheral nervous system. *J. Clin. Invest.* **76**, 1501–1513
- Pitas, R. E., Boyles, J. K., Lee, S. H., Foss, D., and Mahley, R. W. (1987) Astrocyte synthesize apolipoprotein E and metabolize apolipoprotein E-containing lipoproteins. *Biochim. Biophys. Acta* **917**, 148–161
- Nakai, M., Kawamata, T., Taniguchi, T., Maeda, K., and Tanaka, C. (1996) Expression of apolipoprotein E mRNA in rat microglia. *Neurosci. Lett.* **211**, 41–44
- Strittmatter, W. J., Saunders, A. M., Schmechel, D., Pericak-Vance, M., Enghild, J., Salvesen, G. S., and Roses, A. D. (1993) Apolipoprotein E: high-avidity binding to  $\beta$ -amyloid and increased frequency of type 4 allele in late-onset familial Alzheimer disease. *Proc. Natl. Acad. Sci. U.S.A.* **90**, 1977–1981
- Corder, E. H., Saunders, A. M., Strittmatter, W. J., Schmechel, D. E., Gaskell, P. C., Small, G. W., Roses, A. D., Haines, J. L., and Pericak-Vance, M. A. (1993) Gene dose of apolipoprotein E type 4 allele and the risk of Alzheimer's disease in late onset families. *Science* **261**, 921–923
- Namba, Y., Tomonaga, M., Kawasaki, H., Otomo, E., and Ikeda, K. (1991) Apolipoprotein E immunoreactivity in cerebral amyloid deposits and neurofibrillary tangles in Alzheimer's disease and kuru plaque amyloid in Creutzfeldt-Jakob disease. *Brain Res.* **541**, 163–166
- Näslund, J., Thyberg, J., Tjernberg, L. O., Wernstedt, C., Karlström, A. R., Bogdanovic, N., Gandy, S. E., Lannfelt, L., Terenius, L., and Nordstedt, C. (1995) Characterization of stable complexes involving apolipoprotein E and the amyloid  $\beta$  peptide in Alzheimer's disease brain. *Neuron* **15**, 219–228
- Rebeck, G. W., Reiter, J. S., Strickland, D. K., and Hyman, B. T. (1993) Apolipoprotein E in sporadic Alzheimer's disease: allelic variation and receptor interactions. *Neuron* **11**, 575–580
- Jarrett, J. T., Berger, E. P., and Lansbury, P. T., Jr. (1993) The carboxy terminus of the  $\beta$  amyloid protein is critical for the seeding of amyloid formation: implications for the pathogenesis of Alzheimer's disease. *Biochemistry* **32**, 4693–4697
- Lomakin, A., Teplow, D. B., Kirschner, D. A., and Benedek, G. B. (1997) Kinetic theory of fibrillogenesis of amyloid  $\beta$ -protein. *Proc. Natl. Acad. Sci. U.S.A.* **94**, 7942–7947
- Evans, K. C., Berger, E. P., Cho, C. G., Weisgraber, K. H., and Lansbury, P. T., Jr. (1995) Apolipoprotein E is a kinetic but not a thermodynamic inhibitor of amyloid formation: implications for the pathogenesis and treatment of Alzheimer disease. *Proc. Natl. Acad. Sci. U.S.A.* **92**, 763–767
- Naiki, H., Gejyo, F., and Nakakuki, K. (1997) Concentration-dependent inhibitory effects of apolipoprotein E on Alzheimer's  $\beta$ -amyloid fibril formation *in vitro*. *Biochemistry* **36**, 6243–6250
- Walsh, D. M., Lomakin, A., Benedek, G. B., Condron, M. M., and Teplow, D. B. (1997) Amyloid  $\beta$ -protein fibrillogenesis: detection of protofibrillar intermediate. *J. Biol. Chem.* **272**, 22364–22372
- Bitan, G., Lomakin, A., and Teplow, D. B. (2001) Amyloid  $\beta$ -protein oligomerization: prenucleation interactions revealed by photo-induced cross-linking of unmodified proteins. *J. Biol. Chem.* **276**, 35176–35184
- Harper, J. D., Wong, S. S., Lieber, C. M., and Lansbury, P. T. (1997) Observation of metastable A $\beta$  amyloid protofibrils by atomic force microscopy. *Chem. Biol.* **4**, 119–125
- Bitan, G., Kirkitadze, M. D., Lomakin, A., Vollers, S. S., Benedek, G. B., and Teplow, D. B. (2003) Amyloid  $\beta$ -protein (A $\beta$ ) assembly: A $\beta$ 40 and A $\beta$ 42 oligomerize through distinct pathways. *Proc. Natl. Acad. Sci. U.S.A.* **100**, 330–335

## Roles of ApoE in $\beta$ -Amyloidogenesis *In Vitro* and *In Vivo*

19. Lambert, M. P., Barlow, A. K., Chromy, B. A., Edwards, C., Freed, R., Liosatos, M., Morgan, T. E., Rozovsky, I., Trommer, B., Viola, K. L., Wals, P., Zhang, C., Finch, C. E., Krafft, G. A., and Klein, W. L. (1998) Diffusible, nonfibrillar ligands derived from A $\beta$ 1–42 are potent central nervous system neurotoxins. *Proc. Natl. Acad. Sci. U.S.A.* **95**, 6448–6453
20. Nilsberth, C., Westlind-Danielsson, A., Eckman, C. B., Condron, M. M., Axelman, K., Forsell, C., Stenh, C., Luthman, J., Teplow, D. B., Younkin, S. G., Näslund, J., and Lannfelt, L. (2001) The 'Arctic' APP mutation (E693G) causes Alzheimer's disease by enhanced A $\beta$  protofibril formation. *Nat. Neurosci.* **4**, 887–893
21. Hori, Y., Hashimoto, T., Wakutani, Y., Urakami, K., Nakashima, K., Condron, M. M., Tsubuki, S., Saido, T. C., Teplow, D. B., and Iwatsubo, T. (2007) The Tottori (D7N) and English (H6R) familial Alzheimer disease mutations accelerate A $\beta$  fibril formation without increasing protofibril formation. *J. Biol. Chem.* **282**, 4916–4923
22. Hartley, D. M., Walsh, D. M., Ye, C. P., Diehl, T., Vasquez, S., Vassilev, P. M., Teplow, D. B., and Selkoe, D. J. (1999) Protofibrillar intermediates of amyloid  $\beta$ -protein induce acute electrophysiological changes progressive neurotoxicity in cortical neurons. *J. Neurosci.* **19**, 8876–8884
23. Walsh, D. M., Hartley, D. M., Kusumoto, Y., Fezoui, Y., Condron, M. M., Lomakin, A., Benedek, G. B., Selkoe, D. J., and Teplow, D. B. (1999) Amyloid  $\beta$ -protein fibrillogenesis. Structure and biological activity of protofibrillar intermediates. *J. Biol. Chem.* **274**, 25945–25952
24. Morikawa, M., Fryer, J. D., Sullivan, P. M., Christopher, E. A., Wahrle, S. E., DeMattos, R. B., O'Dell, M. A., Fagan, A. M., Lashuel, H. A., Walz, T., Asai, K., and Holtzman, D. M. (2005) Production of astrocyte-derived human apolipoprotein E isoforms from immortalized astrocytes and their interactions with amyloid- $\beta$ . *Neurobiol. Dis.* **19**, 66–76
25. Yamada, K., Yabuki, C., Seubert, P., Schenk, D., Hori, Y., Ohtsuki, S., Terasaki, T., Hashimoto, T., and Iwatsubo, T. (2009) A $\beta$  immunotherapy: intracerebral sequestration of A $\beta$  by an anti-A $\beta$  monoclonal antibody 266 with high-affinity to soluble A $\beta$ . *J. Neurosci.* **29**, 11393–11398
26. Meyer-Luehmann, M., Coomaraswamy, J., Bolmont, T., Kaeser, S., Schaefer, C., Kilger, E., Neuenschwander, A., Abramowski, D., Frey, P., Jaton, A. L., Vigouret, J. M., Paganetti, P., Walsh, D. M., Mathews, P. M., Ghiso, J., Staufenbiel, M., Walker, L. C., and Jucker, M. (2006) Exogenous induction of cerebral  $\beta$ -amyloidogenesis is governed by agent and host. *Science* **313**, 1781–1784
27. Hashimoto, T., Wakabayashi, T., Watanabe, A., Kowa, H., Hosoda, R., Nakamura, A., Kanazawa, I., Arai, T., Takio, K., Mann, D. M., and Iwatsubo, T. (2002) CLAC: a novel Alzheimer amyloid plaque component derived from a transmembrane precursor, CLAC-P/collagen type XXV. *EMBO J.* **21**, 1524–1534
28. Kane, M. D., Lipinski, W. J., Callahan, M. J., Bian, F., Durham, R. A., Schwarz, R. D., Roher, A. E., and Walker, L. C. (2000) Evidence for seeding of  $\beta$ -amyloid by intracerebral infusion of Alzheimer brain extracts in  $\beta$ -amyloid precursor protein-transgenic mice. *J. Neurosci.* **20**, 3606–3611
29. Ribalta, J., Vallvé, J. C., Girona, J., and Masana, L. (2003) Apolipoprotein and apolipoprotein receptor genes, blood lipids and disease. *Curr. Opin. Clin. Nutr. Metab. Care* **6**, 177–187
30. Hashimoto, T., Serrano-Pozo, A., Hori, Y., Adams, K. W., Takeda, S., Banerji, A. O., Mitani, A., Joyner, D., Thyssen, D. H., Bacskaï, B. J., Frosch, M. P., Spires-Jones, T. L., Finn, M. B., Holtzman, D. M., and Hyman, B. T. (2012) Apolipoprotein E, especially apolipoprotein E4, increases the oligomerization of amyloid  $\beta$  peptide. *J. Neurosci.* **32**, 15181–15192
31. Aleshkov, S., Abraham, C. R., and Zannis, V. I. (1997) Interaction of nascent ApoE2, ApoE3, and ApoE4 isoforms expressed in mammalian cells with amyloid peptide  $\beta$  (1–40): relevance to Alzheimer's disease. *Biochemistry* **36**, 10571–10580
32. LaDu, M. J., Falduto, M. T., Manelli, A. M., Reardon, C. A., Getz, G. S., and Frail, D. E. (1994) Isoform-specific binding of apolipoprotein E to  $\beta$ -amyloid. *J. Biol. Chem.* **269**, 23403–23406
33. Yang, D. S., Smith, J. D., Zhou, Z., Gandy, S. E., and Martins, R. N. (1997) Characterization of the binding of amyloid- $\beta$  peptide to cell culture-derived apolipoprotein E2, E3, and E4 isoforms and to isoforms from human plasma. *J. Neurochem.* **68**, 721–725
34. Gomez-Isla, T., West, H. L., Rebeck, G. W., Harr, S. D., Growdon, J. H., Locascio, J. J., Perls, T. T., Lipsitz, L. A., and Hyman, B. T. (1996) Clinical and pathological correlates of apolipoprotein E  $\epsilon$ 4 in Alzheimer's disease. *Ann. Neurol.* **39**, 62–70
35. Holtzman, D. M., Bales, K. R., Tenkova, T., Fagan, A. M., Parsadanian, M., Sartorius, L. J., Mackey, B., Olney, J., McKeel, D., Wozniak, D., and Paul, S. M. (2000) Apolipoprotein E isoform-dependent amyloid deposition and neuritic degeneration in a mouse model of Alzheimer's disease. *Proc. Natl. Acad. Sci. U.S.A.* **97**, 2892–2897
36. Fagan, A. M., Watson, M., Parsadanian, M., Bales, K. R., Paul, S. M., and Holtzman, D. M. (2002) Human and murine ApoE markedly alters A $\beta$  metabolism before and after plaque formation in a mouse model of Alzheimer's disease. *Neurobiol. Dis.* **9**, 305–318
37. Tai, L. M., Bilousova, T., Jungbauer, L., Roeske, S. K., Youmans, K. L., Yu, C., Poon, W. W., Cornwell, L. B., Miller, C. A., Vinters, H. V., Van Eldik, L. J., Fardo, D. W., Estus, S., Bu, G., Glyys, K. H., and Ladu, M. J. (2013) Levels of soluble apolipoprotein E/amyloid- $\beta$  (A $\beta$ ) complex are reduced and oligomeric A $\beta$  increased with APOE4 and Alzheimer disease in a transgenic mouse model and human samples. *J. Biol. Chem.* **288**, 5914–5926
38. Tai, L. M., Mehra, S., Shete, V., Estus, S., Rebeck, G. W., Bu, G., and LaDu, M. J. (2014) Soluble apoE/A $\beta$  complex: mechanism and therapeutic target for APOE4-induced AD risk. *Mol. Neurodegener.* **9**, 2
39. Dong, L. M., Wilson, C., Wardell, M. R., Simmons, T., Mahley, R. W., Weisgraber, K. H., and Agard, D. A. (1994) Human apolipoprotein E: role of arginine 61 in mediating the lipoprotein preferences of the E3 and E4 isoforms. *J. Biol. Chem.* **269**, 22358–22365
40. Dong, L. M., and Weisgraber, K. H. (1996) Human apolipoprotein E4 domain interaction: arginine 61 and glutamic acid 255 interact to direct the preference for very low density lipoproteins. *J. Biol. Chem.* **271**, 19053–19057
41. Bentley, N. M., Ladu, M. J., Rajan, C., Getz, G. S., and Reardon, C. A. (2002) Apolipoprotein E structural requirements for the formation of SDS-stable complexes with  $\beta$ -amyloid-(1–40): the role of salt bridge. *Biochem. J.* **366**, 273–279
42. Englund, H., Sehlin, D., Johansson, A. S., Nilsson, L. N., Gellerfors, P., Paulie, S., Lannfelt, L., and Pettersson, F. E. (2007) Sensitive ELISA detection of amyloid- $\beta$  protofibrils in biological samples. *J. Neurochem.* **103**, 334–345
43. Lord, A., Englund, H., Söderberg, L., Tucker, S., Clausen, F., Hillered, L., Gordon, M., Morgan, D., Lannfelt, L., Pettersson, F. E., and Nilsson, L. N. (2009) Amyloid- $\beta$  protofibril levels correlate with spatial learning in Arctic Alzheimer's disease transgenic mice. *FEBS J.* **276**, 995–1006
44. Cheng, I. H., Palop, J. J., Esposito, L. A., Bien-Ly, N., Yan, F., and Mucke, L. (2004) Aggressive amyloidosis in mice expressing human amyloid peptides with the Arctic mutation. *Nat. Med.* **10**, 1190–1192
45. Bu, G. (2009) Apolipoprotein E and its receptors in Alzheimer's disease: pathways, pathogenesis and therapy. *Nat. Rev. Neurosci.* **10**, 333–344
46. Bales, K. R., Verina, T., Dodel, R. C., Du, Y., Altstiel, L., Bender, M., Hyslop, P., Johnstone, E. M., Little, S. P., Cummins, D. J., Piccardo, P., Ghetti, B., and Paul, S. M. (1997) Lack of apolipoprotein E dramatically reduces amyloid  $\beta$ -peptide deposition. *Nat. Genet.* **17**, 263–264
47. DeMattos, R. B., Cirrito, J. R., Parsadanian, M., May, P. C., O'Dell, M. A., Taylor, J. W., Harmony, J. A., Aronow, B. J., Bales, K. R., Paul, S. M., and Holtzman, D. M. (2004) ApoE and clusterin cooperatively suppress A $\beta$  level and deposition: evidence that apoE regulates extracellular A $\beta$  metabolism *in vivo*. *Neuron* **41**, 193–202